ELSEVIER

Cardiovascular Research 62 (2004) 500–508

Cardiovascular Research

www.elsevier.com/locate/cardiores

Gene dose-dependent atrial arrhythmias, heart block, and brady-cardiomyopathy in mice overexpressing A_3 adenosine receptors

Larissa Fabritz[a,*,1], Paulus Kirchhof[a,*,1], Lisa Fortmüller[a], John A. Auchampach[b], Hideo A. Baba[c], Günter Breithardt[a], Joachim Neumann[d], Peter Boknik[d], Wilhelm Schmitz[d]

[a] *Department of Cardiology and Angiology and Institute for Arteriosclerosis Research, University Hospital Münster, Münster, Germany*
[b] *Department of Pharmacology and Cardiovascular Research Center, Medical College of Wisconsin, Milwaukee, WI, USA*
[c] *Institute of Pathology, University of Essen, Essen, Germany*
[d] *Institute of Pharmacology and Toxicology, University Hospital Münster, Münster, Germany*

Received 6 December 2003; received in revised form 31 January 2004; accepted 4 February 2004

Time for primary review 30 days

Available online 16 March 2004

Abstract

Objective: An increased expression of adenosine receptors is a promising target for gene therapy aimed at protecting the myocardium against ischemic damage, but may alter cardiac electrophysiology. We therefore studied the effects of heart-directed overexpression of A_3 adenosine receptors (A_3ARs) at different gene doses on sinus and atrio-ventricular (AV) nodal function in mice. **Methods and results:** Mice with heart-specific overexpression of A_3AR at high (A_3^{high}) or low (A_3^{low}) levels and their wild-type littermates were studied. Telemetric electrocardiogram (ECG) recordings in adult freely moving A_3^{high} mice showed profound sinus bradycardia resulting in either ventricular escape rhythms or an incessant bradycardia–tachycardia syndrome (minimal heart rate A_3^{high} 217 ± 25*; WT 406 ± 21 beats/min, all values as mean ± S.E.M., $n = 7$ per genotype, $*p < 0.05$). Exercise attenuated bradycardia in A_3^{high} mice (maximal heart rate A_3^{high} 650 ± 13*; WT 796 ± 13 beats/min) and first-degree AV nodal block was present (PQ interval A_3^{high} 36 ± 4*; WT 23 ± 5 ms). Isolated hearts showed complete heart block (10/17 A_3^{high}* vs. 1/17 WT). Atrial bradycardia and AV block were already present 3 weeks after birth. Doppler echocardiography revealed atrial dysfunction and progressive atrial enlargement that was moderate at 3 and 8 weeks, and progressed at 12 and 21 weeks of age (all $p < 0.05$ vs. WT). Atrial contractility and sarcoendoplasmic Ca^{2+} ATPase (SERCA) 2a protein expression were reduced in isolated left A_3^{high} atria at the age of 14 weeks. Fibrosis was present in left A_3^{high} atria at 14 weeks, but not at 5 weeks of age. A_3^{low} mice had first-degree AV block without arrhythmias or structural changes. **Conclusions:** Heart-directed overexpression of A_3AR resulted in gene dose-dependent AV block and pronounced sinus nodal dysfunction in vivo. Profound bradycardia heralded atrial and ventricular dilatation, dysfunction, and fibrosis. In contrast to A_1 adenosine receptors (A_1AR), the effects of A_3AR overexpression were attenuated during exercise. This may have implications for the physiology of sinus nodal regulation and for therapeutic attempts to increase the expression of adenosine receptors.

Keywords: Integrative physiology; Heart rate regulation; Autonomous nervous system; Sinus node dysfunction; AV block; Atrial cardiomyopathy; A_3 adenosine receptor; Transgenic mice

1. Introduction

Heart rate is determined by the depolarization rate of pacemaker cells in the sinus node [1,2]. The ionic currents that depolarize pacemaker cells can be modulated, for example, by β-adrenoreceptors, muscarinic receptors, and adenosine receptors. We have recently reported that heart-directed overexpression of A_1 adenosine receptors (A_1ARs) causes a decreased chronotropic response to exercise and first-degree atrio-ventricular (AV) nodal block [3]. In addi-

Abbreviations: A_3AR, A_3 adenosine receptor; A_1AR, A_1 adenosine receptor; A_3^{high}, mice with heart-directed high-level overexpression of A_3AR; A_3^{low}, mice with heart-directed low-level overexpression of A_3AR; AV, atrio-ventricular; ECG, electrocardiogram; SERCA, sarcoendoplasmic Ca^{2+} ATPase

* Corresponding authors. Medizinische Klinik und Poliklinik C, Kardiologie und Angiologie, Universitätsklinikum Münster, Albert-Schweitzer-Straße 33, Münster D-48129, Germany. Tel.: +49-251-8347638; fax: +49-251-8347864.

E-mail addresses: kirchhp@uni-muenster.de (P. Kirchhof), fabritzl@uni-muenster.de (L. Fabritz).

[1] Contributed equally.

0008-6363/$ - see front matter © 2004 European Society of Cardiology. Published by Elsevier B.V. All rights reserved.
doi:10.1016/j.cardiores.2004.02.004

tion to A_1AR, A_3 adenosine receptors (A_3ARs) are expressed in the human heart [4] and their pharmacological stimulation modulates cardiac function [5]. Heart-directed overexpression of A_3AR in mice protects the heart against ischemia, but may also cause ventricular dysfunction and bradycardia at high levels of overexpression [6]. As pharmacological treatment with A_3AR agonists [7] and gene therapy with targeted A_3AR expression [6,8] have been proposed to protect the myocardium against ischemic events, electrophysiological effects of A_3AR overexpression may have physiological and clinical relevance.

Here, we report that heart-directed high-level overexpression of A_3AR causes severe sinus node dysfunction at rest, bradycardia–tachycardia syndrome, and complete AV block in vivo in mice. Exercise attenuates bradycardia and AV block. Electrophysiological changes accompany atrial and ventricular dysfunction and fibrosis. Low-level overexpression of A_3AR, in contrast, only results in first-degree AV block at rest. A_1AR and A_3AR differentially affect sinus nodal and AV nodal function. High-level overexpression of A_3AR may cause brady-cardiomyopathy.

2. Methods

Transgenic mice were bred from transgenic mouse lines with heart-directed (α-MHC promoter) overexpression of A_3AR, as described in Ref. [6]. The two mouse lines used expressed about 13 fmol (A_3^{low}) or about 67 fmol/mg (A_3^{high}) high-affinity Gi-coupled A_3AR per milligram of protein [6]. All experiments conformed to the Guide for the Care and Use of Laboratory Animals published by the US National Institutes of Health (NIH Publication No. 85-23, revised 1996) and were approved by the local animal care committee.

2.1. Electrocardiogram (ECG) measurements in sedated mice

Mice were sedated by intraperitoneal application of ketamine/xylazine (50 mg/20 mg mixture) at 16 weeks and urethane (2 g/kg body weight) at 18 weeks of age. Gel-covered silver wire loops were attached around the four limbs of the animals to record a six-lead surface ECG. Signals were preamplified and displayed on paper (amplitude 20 mV/mm, paper speed 100 mm/s; Siemens Megacart, Erlangen, Germany) [3].

2.2. ECG recordings in awake mice

Sixteen-week-old mice were instrumented with a telemetric ECG transmitter (Data Science, Minneapolis, USA) and lead II of the ECG was continuously recorded via two subcutaneous electrodes [3,9]. In addition, we recorded short strips of surface ECGs in nonsedated 3-week-old pairs of A_3^{high} and WT mice using flexible silver wire loops that were gently placed around the limbs of the animals. After a postoperative recovery period of 10 days, telemetric ECG recordings were obtained in freely moving mice during normal activity and during a standardized exercise protocol that has been described in detail before [3]. In brief, the telemetric ECG was first continuously recorded for 1 h during daytime. Mice were then placed in a water-filled tank for 6 min (20×30 cm width, 15 cm depth, water temperature 34 °C). After this submaximal exercise [3,10], mice were put back into their cages. The ECG was continuously recorded during swimming and for 55 min after swimming. In addition, 24-h periods of telemetric ECG recordings were analyzed for arrhythmias. Littermate pairs of WT and transgenic mice were simultaneously subjected to the protocol.

2.3. Isolated heart measurements

Isolated Langendorff-perfused mouse hearts of mice aged 40 ± 3 weeks were studied using published techniques [3,11]. In brief, hearts were rapidly excised and perfused on a vertical Langendorff apparatus (Hugo Sachs Harvard Apparatus, March-Hugstetten, Germany) at a constant perfusion pressure of 90–100 mm Hg (flow rate 4 ± 1 ml/min) [12]. An octapolar murine electrophysiology catheter (CI'BER mouse; NuMED, Hopkinton, NY, USA) was inserted into the right atrium and right ventricle. The perfused and instrumented heart was allowed to stabilize for 10 min. Thereafter, spontaneous rhythm was observed for 5 min. The right atrium was paced at constant heart rates (150–750 beats/min, 1.5 min of pacing per heart rate) via the octapolar catheter. Incremental atrial pacing was performed to test the antegrade conduction properties of the AV node. The pacing protocol was repeated during infusion of orciprenaline (1.4 μmol/l continuous infusion) [3].

2.4. Isolated atria

Atria were isolated from 14-week-old animals of either genotype and superfused in a tissue bath using repeatedly published methods (e.g., Ref. [13]). Left atrial preparations were electrically stimulated to assess atrial contractility. Right atrial preparations were superfused to assess spontaneous rate of contraction. The A_3AR agonist N^6-(3-iodobenzyl)-adenosine-5′ -*N*-methyluronamide (IB MECA; Tocris Cookson, Ellisville, MO, USA) or the α,β-adrenoreceptor agonist isoproterenol were applied for 10 min at different concentrations.

2.5. ECG analysis

All analyses were performed blinded to genotype. Surface ECG recordings were manually analyzed for heart rate, PQ, QRS, and QT intervals. Telemetric ECG recordings were digitally analyzed for heart rate and PQ intervals during 5-min periods of normal activity, during the swimming period,

and during 5 min, 1 h after the beginning of swimming. The program automatically determined RR intervals; all computed intervals were verified manually. PQ intervals were compared during periods of equal heart rate. All recordings were manually reviewed for arrhythmias. Isolated heart recordings were analyzed for atrial and ventricular rate, presence of higher-degree AV block, and AV nodal conduction times measured as the time from the latest atrial activation to the earliest ventricular activation [3].

2.6. Histology and protein biochemistry

Hearts were rapidly excised, immersed in formalin, and stained using Sirius red stains. Atrial cell diameter was measured in 100 cells at the height of the nucleus. Additional right and left atrial tissue samples were shock-frozen and prepared for protein biochemistry [14]. We analyzed the protein level of phospholamban, calsequestrin, and sarcoendoplasmic Ca^{2+} ATPase (SERCA; SERCA and calsequestrin antibodies were kind gifts of Dr. L.R. Jones, Indianapolis, IN, USA) in atrial and ventricular preparations.

2.7. Doppler echocardiography

Sedated (intraperitoneal application of ketamine S 32 mg/kg body weight and xylazine 13 mg/kg body weight) pairs of mice were studied using a Sonos 5500 echocardiography system equipped with a 15-MHz linear transducer and a 12-MHz Doppler transducer (Philips Medical Systems) using published techniques [3]. The left atrium was visualized in the parasternal long axis in the plane of the aortic root, and the left atrial diameter was measured during ventricular systole at its maximal dimension in five 2D and M-mode images. Atrial function was assessed using transmitral Doppler flow measurements. Operators were blinded to genotype.

2.8. Statistics

Variables were compared between genotypes by post-hoc Student's *t* test and ANOVA analyses using statistical software (SPSS and Excel). Incidences of AV block and arrhythmias were compared using Fisher's exact test. Two-

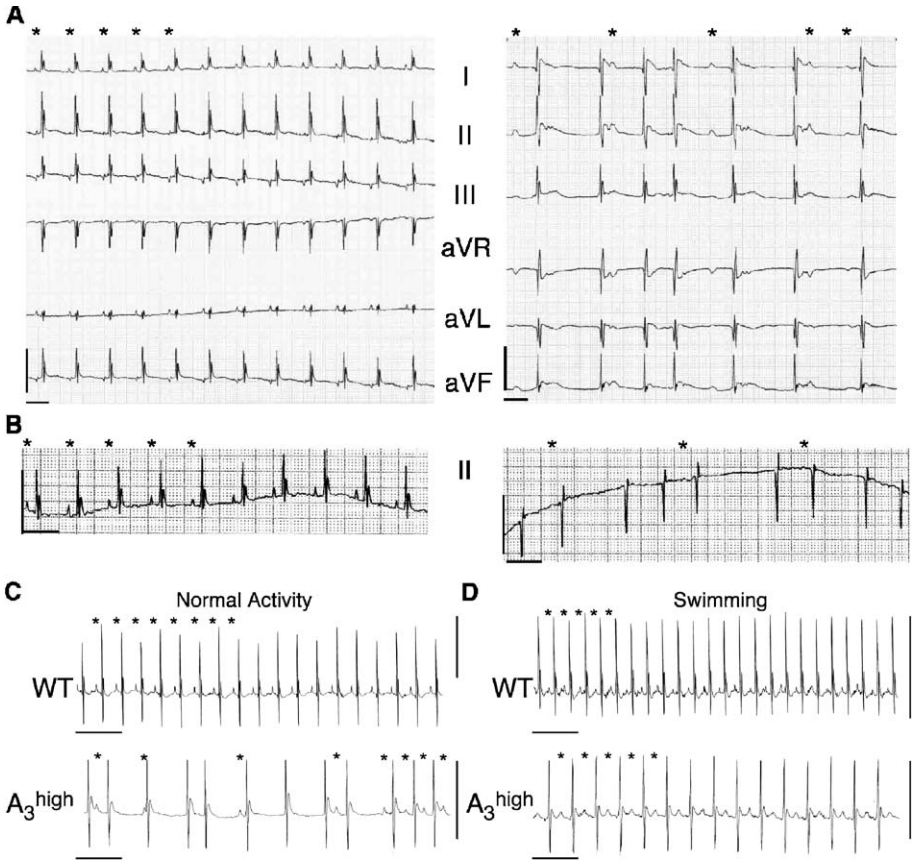

Fig. 1. Sinus node dysfunction, AV block, and atrial arrhythmias in A_3^{high} mice. (A) Six-lead surface ECG recording from a wild-type (left) and A_3^{high} mouse (right) at 18 weeks of age. Marked right atrial bradyarrhythmia results in ventricular escape beats in the A_3^{high} mouse. Asterisks (*) indicate P waves. (B) Lead II of a representative surface ECG recording from a nonsedated wild-type (left panel) and A_3^{high} mouse (right panel) at 3 weeks of age. (C) Representative telemetric ECG recording from a freely moving WT and A_3^{high} mouse during normal activity at 18 weeks of age. Marked sinus bradycardia is followed by a run of atrial tachycardia. The ventricular rate is determined by ventricular escape beats. (D) Representative telemetric ECG recording from a freely moving WT and A_3^{high} mouse during swimming exercise. The A_3^{high} mouse shows sinus bradycardia and first-degree AV block.

sided p values <0.05 were considered significant and are marked by an asterisk (*). Continuous variables are reported as mean ± S.E.M.

3. Results

3.1. Atrial arrhythmias in A_3^{high} mice in vivo

Freely moving and sedated 16- and 18-week-old A_3^{high} mice ($n=7$ per genotype) showed severe sinus bradycardia and repetitive episodes of atrial arrhythmias during normal activity, which were not present in WT animals (Fig. 1A and C, $p<0.05$). We hardly found periods of normal sinus rhythm during telemetric ECG recording in sedentary A_3^{high} mice. Nonsedated A_3^{high} mice already showed marked bradycardia alternating with atrial arrhythmias during short strips of six-lead ECG recordings at the age of 3 weeks ($n=4$ A_3^{high} and 4 WT, $p<0.05$; Fig. 1B). There were no arrhythmias 5 days after birth ($n=5$ A_3^{high} and 5 WT).

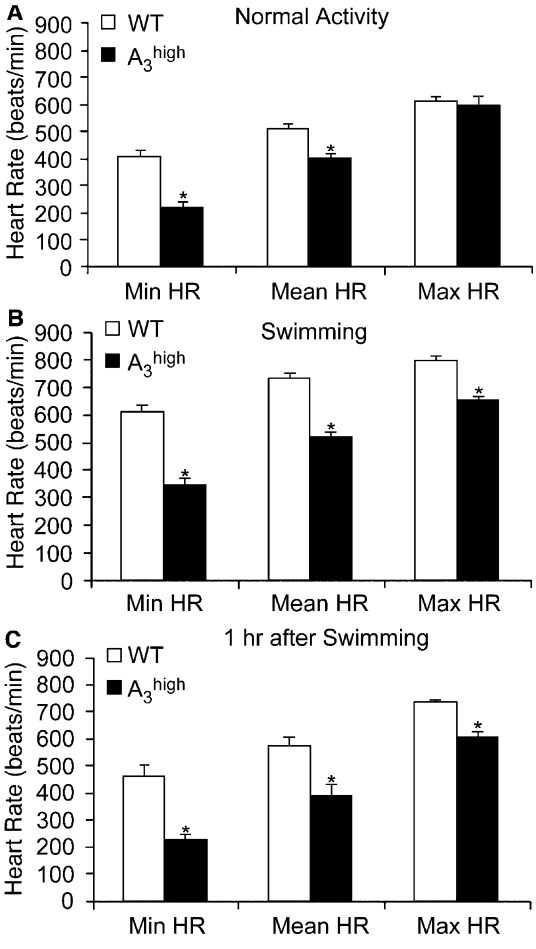

Fig. 2. Marked resting bradycardia is attenuated during exercise in conscious A_3^{high} mice. Minimal, mean, and maximal heart rates are given for WT (open bars, $n=7$) and TG mice (filled bars, $n=7$) during normal activity (A), swimming exercise (B), and 1 h after swimming (C). Asterisks (*) indicate significant differences between A_3^{high} and WT mice.

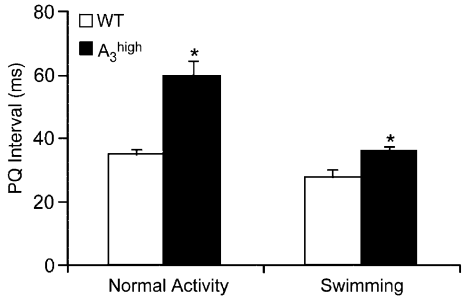

Fig. 3. Prolonged PQ interval in conscious A_3^{high} mice. Mean PQ interval during exercise in wild-type (open bars, $n=7$) and A_3^{high} mice (filled bars, $n=7$). Asterisks (*) indicate significant differences between TG and wild type. During normal activity, PQ intervals could not be determined in vivo due to marked sinus bradycardia.

3.2. Bradycardia in vivo

Adult (18 weeks old) sedated A_3^{high} animals had lower heart rates, prolonged PQ intervals, and longer QT intervals than littermate WT. Heart rate was already lower 3 weeks after birth (A_3^{high} 434 ± 25 beats/min, WT 655 ± 9 beats/

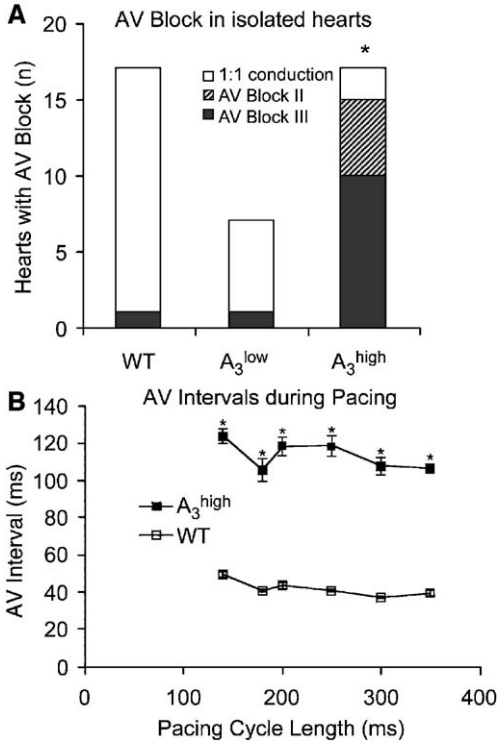

Fig. 4. Bradycardia, AV block, and atrial tachyarrhythmias in isolated hearts of A_3^{high} mice. (A) Incidence of AV nodal block in isolated WT and A_3^{high} mouse hearts. Shown is the presence of complete heart block (AV block III, black bars), second-degree AV block (AV block II, striped bars), and hearts without higher-degree AV block (open bars). Asterisks indicate significant differences between WT and A_3^{high} hearts. (B) Mean AV intervals in isolated WT and TG hearts during atrial pacing measured in hearts without higher-degree AV nodal block. AV interval (ordinate) is plotted vs. pacing cycle length (abscissa) for wild-type (open boxes) and A_3^{high} mouse hearts (filled boxes). Asterisks (*) indicate significant differences between A_3^{high} and WT hearts.

min, $n=4$ per genotype, $p<0.01$) and 2 weeks after birth (A_3^{high} 520 ± 40 beats/min, $n=5$; WT 681 ± 31 beats/min, $n=5$, $p=0.02$).

Minimal heart rate was markedly depressed. Maximal heart rate was not reduced in A_3^{high} mice during normal activity (Fig. 2). During exercise and recovery from exercise, a regular supraventricular rhythm was present in A_3^{high} mice, albeit with persistent sinus bradycardia (Figs. 1D and 2).

3.3. AV nodal function in vivo

In A_3^{high} mice, AV nodal conduction could often not be determined during normal activity due to lower heart rates in the atrium than in the ventricle (Fig. 1). Intermittently, complete AV block was observed in freely moving A_3^{high} mice during normal activity. During exercise, all A_3^{high} mice developed supraventricular rhythms with 1:1 conduction, albeit with marked PQ prolongation (Figs. 1D and 3).

A_3^{low} mice showed a slight prolongation of the PQ interval (sedated mice: A_3^{low} 42 ± 2 ms, WT 37 ± 1 ms, $n=6$ per group, $p<0.05$; freely moving mice: A_3^{low} 37.9 ± 1.0 ms at heart rates of 467 ± 12 beats/min; WT 34.9 ± 0.7 ms at heart rates of 460 ± 7 beats/min, $p<0.05$). The other ECG parameters were not different between A_3^{low} and WT mice (data not shown).

3.4. Electrophysiology in isolated hearts and atria

To assess AV nodal conduction at comparable atrial heart rates and to measure intrinsic heart rate [15] and intrinsic AV conduction in the intact heart deprived of autonomic influences, we studied isolated Langendorff-perfused hearts of adult A_3^{high} ($n=17$), A_3^{low} ($n=7$), and WT ($n=17$) mice during spontaneous rhythm and atrial pacing. This setup allows reproducible measurement of spontaneous, intrinsic heart rate (mean heart rates between 423 and 462 beats/min

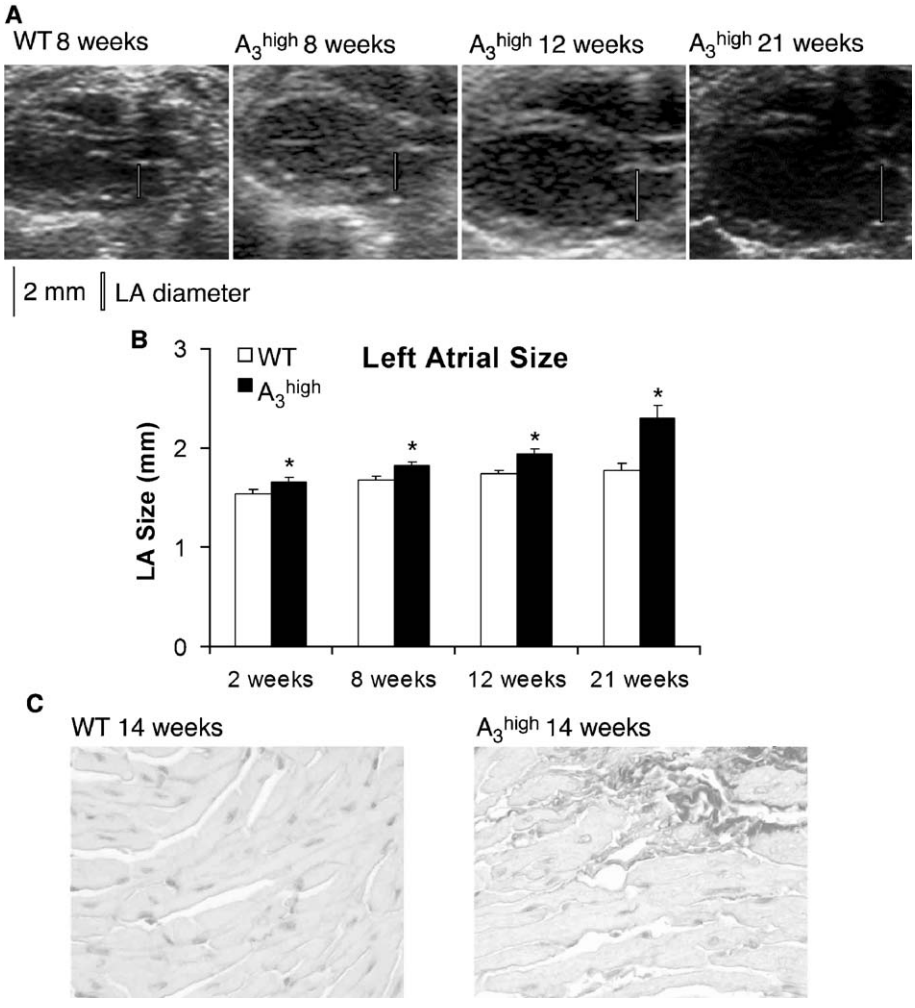

Fig. 5. Atrial dilatation and fibrosis in A_3^{high} mice. (A) Representative echocardiographic parasternal long axis views of a WT mouse heart and A_3^{high} mouse hearts at 8, 12, and 21 weeks of age. White bars indicate the left atrial diameter. (B) Mean left atrial diameter in WT (open bars) and A_3^{high} mice (filled bars). Asterisks (*) indicate significant differences between A_3^{high} and WT. For other echocardiographic parameters, see Table 2. (C) Sirius red staining of left atria from littermates aged 14 weeks indicating fibrosis in A_3^{high} atria.

Table 1
Gravimetric and biochemical protein measurements in left atrial and ventricular samples of wild-type (WT) and A_3^{high} mice aged 14 weeks

Gravimetric measurements	WT ($n=15$)	A_3^{high} ($n=10$)
Body weight (g)	27.82 ± 0.71	26.54 ± 1.05
Left atrial weight (mg)	5.53 ± 0.26	9.92 ± 0.5*
Left atrial weight/body weight ratio (mg/g)	0.199 ± 0.008	0.378 ± 0.024*
Left ventricular weight (mg)	118.33 ± 2.84	118.48 ± 5.23
Left ventricular weight/body weight ratio (mg/g)	4.26 ± 0.07	4.47 ± 0.12
Protein biochemistry	**WT ($n=6$)**	**A_3^{high} ($n=6$)**
Atrial phospholamban (arbitrary units)	101.7 ± 13.4	80.2 ± 15.2
Atrial phospholamban/calsequestrin ratio	0.047 ± 0.008	0.050 ± 0.010
Atrial SERCA (arbitrary units)	5599.99 ± 592.71	1742.17 ± 679.85*
Atrial SERCA/calsequestrin ratio	2.65 ± 0.5	0.94 ± 0.26*
Ventricular phospholamban (arbitrary units)	160,433 ± 3664	150,950 ± 3798
Ventricular PLB/calsequestrin ratio	0.054 ± 0.04	0.047 ± 0.002
Ventricular SERCA (arbitrary units)	7,437,924 ± 514,045	4,230,801 ± 290,231*
Ventricular SERCA/calsequestrin ratio	2.54 ± 0.37	1.31 ± 0.11*

* Indicates significant differences between WT and A3high mice. SERCA, sarco-endoplasmic reticulum ATPase II; PLB, phospholamban.

in wild-type hearts in previous studies) [3,11,12]. Spontaneous atrial rate was lower in A_3^{high} than in WT hearts (A_3^{high} 245 ± 19 beats/min; WT 423 ± 28 beats/min, $p<0.05$). Ten of 17 A_3^{high} hearts showed complete AV block (Fig. 4A). The β-adrenoreceptor agonist orciprenaline (1.4 μmol/l) accelerated atrial rate in WT hearts but not in A_3^{high} hearts (A_3^{high} 170 ± 25 beats/min; WT 618 ± 34 beats/min, $p<0.05$ between genotypes). As ventricular rates were higher than atrial rates in A_3^{high} hearts during orciprenaline infusion (mean ventricular rate 325 ± 28 beats/min), recovery from AV block could not be assessed reliably. Three A_3^{high} hearts developed spontaneous episodes of atrial fibrillation. In A_3^{low} hearts, heart rate was not different from WT during baseline and, like WT, was accelerated by orciprenaline (A_3^{low} from 423 ± 14 to 561 ± 20, $p<0.05$ for drug vs. baseline).

In those seven A_3^{high} hearts without complete AV block, AV conduction times were prolonged (Fig. 4B) and antegrade AV nodal conduction was slower during incremental atrial pacing (Wenckebach point: A_3^{high} 160 ± 18 ms, WT 79 ± 3 ms, $p<0.05$). Antegrade AV nodal conduction was not altered in A_3^{low} hearts (Wenckebach point A_3^{low} 76 ± 2 ms, $n=7$).

Spontaneously beating right atria (14 weeks of age) showed bradyarrhythmias in all A_3^{high} preparations studied. Spontaneous beating rates were not decreased in A_3^{low} (WT 354 ± 7 beats/min, A_3^{low} 351 ± 26 beats/min). The A_3AR agonist IB MECA (10^{-7} M) reduced spontaneous rates in A_3^{low} (286 ± 36 beats/min), but not in WT atria (352 ± 13 beats/min, $n=7$, $p<0.05$).

3.5. Atrial morphology and contractile function

Atrial size was measured in WT and A_3^{high} mice at the age of 2 weeks (7 pairs), 8 weeks (14 pairs), 12 weeks (13 pairs), and 21 weeks (10 pairs) by serial echocardiography: Atrial size was increased by 10% in A_3^{high} mice at the age of 2 and 8 weeks and further increased at the age of 12 and 21 weeks (Fig. 5), concordant with gravimetric results (Table 1). The peak of the atrial wave of transmitral Doppler flow, generated by the contraction of the left atrium, was diminished at 8 weeks of age in A_3^{high} mice (Table 2). Histologically, we found atrial fibrosis in A_3^{high} atria at the age of 14 weeks (Fig. 5), but not at the age of 5 weeks ($n=3$), except for the right atrium of one mouse at 5 weeks with extreme bradyarrhythmia. Diameter of atrial cells was unaltered in A_3^{high} at the age of 5 weeks (data not shown). Ventricular contractile function as assessed by M-mode echocardiography was normal in A_3^{high} mice at 8 weeks, but reduced at 21 weeks of age (Table 2). Atrial and ventricular morphology

Table 2
Atrial and ventricular biplane, M-mode, and Doppler echocardiographic measurements in WT and A_3^{high} mice

	8 weeks		21 weeks	
	WT ($n=14$)	A_3^{high} ($n=14$)	WT ($n=10$)	A_3^{high} ($n=10$)
Heart rate (beats/min)	330 ± 12	303 ± 9	312 ± 16	272 ± 16
AoV (mm)	1.35 ± 0.02	1.34 ± 0.02	1.35 ± 0.02	1.37 ± 0.02
MV E-wave peak (cm/s)	72.7 ± 2.4	73.7 ± 3.0	65.9 ± 3.4	67.1 ± 3.1
MV A-wave peak (cm/s)	35.7 ± 2.5	28.3 ± 1.9*	29.1 ± 1.8	23.4 ± 1.6*
MV E/A	2.14 ± 0.14	2.71 ± 0.17*	2.33 ± 0.19	2.97 ± 0.20*
LVEDD (mm)	4.00 ± 0.06	4.22 ± 0.08*	3.92 ± 0.07	4.67 ± 0.13*
LVESD (mm)	2.44 ± 0.04	2.66 ± 0.07*	2.39 ± 0.04	3.02 ± 0.07*
FS (%)	38.9 ± 0.8	37.1 ± 0.7	38.9 ± 1.0	35.4 ± 0.8*
Vcf (circ/s)	4.9 ± 0.19	4.6 ± 0.19	4.9 ± 0.2	4.5 ± 0.3
Corrected Vcf (circ/s)	11.5 ± 0.6	10.4 ± 0.5	11.2 ± 0.6	9.6 ± 0.6#
Stroke volume (μl)	32 ± 7	34 ± 8	28 ± 7	34 ± 9
Body weight (g)	25.0 ± 0.9	25.0 ± 0.8	29.1 ± 1.1	31.3 ± 0.9

Bradycardic episodes of WT were selected for analysis in order to compare recordings during similar heart rates.
LA, left atrial diameter; AoV, aortic valve diameter; MV, mitral valve; E/A, ratio of early to atrial wave; LVEDD, left ventricular end-diastolic diameter; LVESD, left ventricular end-systolic diameter; FS, fractional shortening; corrected Vcf, velocity of circumferential fiber shortening divided by the square root of the RR interval (s).
Stroke volume was calculated as the product of Doppler aortic flow velocity time integral (cm) and area of the left ventricular outflow tract (mm^2). Values were intermediate at the age of 12 weeks.
* Indicates significant differences between A_3^{high} and WT.
# $p=0.08$.

and function as assessed by echocardiography ($n=7$ per group) were normal in A_3^{low} hearts (12 weeks old).

Basal force of contraction was reduced in electrically stimulated left atria from A_3^{high} mice (14 weeks old, A_3^{high} 1.03 ± 0.13 mN, $n=10$ vs. WT 2.08 ± 0.31 mN, $n=8$), but not in A_3^{low} (14 weeks old, 1.78 ± 0.26 mN, $n=5$). The A_3AR agonist IB MECA reduced force of contraction in both A_3^{low} (1.22 ± 0.4 mN, $p<0.05$ vs. WT and vs. A_3^{high}) and A_3^{high} (0.52 ± 0.09 mN, $p<0.05$ vs. WT and vs. A_3^{low}) compared to WT atria (2.20 ± 0.24 mN) at concentrations of 10^{-7} M and higher, values given for 10^{-7} M. The maximum contractile response to isoproterenol was attenuated in isolated atria from both A_3^{low} and A_3^{high} mice (WT 5.2 ± 0.4 mN or $184 \pm 9\%$ of control, A_3^{low} 3.1 ± 0.3 mN or $147 \pm 6\%$ of control, A_3^{high} 2.4 ± 3.5 mN or $135 \pm 17\%$ of control, $n=8$ per group, values given for isoproterenol concentrations of 10^{-5} M, $p<0.05$ vs. WT). Similar to findings in models of heart failure, expression of SERCA was decreased in A_3^{high} atria and ventricles compared to age-matched WT at the age of 14 weeks (Table 1), but not altered in atria from A_3^{low} hearts compared to WT.

4. Discussion

4.1. Main findings

Heart-directed high-level overexpression of A_3AR in mice caused profound resting bradycardia, AV block, and incessant bradycardia–tachycardia syndrome. These electrophysiological effects were attenuated during exercise. Low-level A_3 adenosine receptor overexpression only caused mild AV nodal conduction delay during periods of low autonomic tone. Atrial arrhythmias heralded atrial and ventricular cardiomyopathy, suggestive of a brady-cardiomyopathy. These findings have implications for the physiology of sinus nodal regulation and for gene therapy aimed at increasing the function of adenosine receptors.

4.2. Bradycardia–tachycardia syndrome

The sinus node hardly contributed to heart rate in A_3^{high} mice during normal activity in vivo. Rather, profound atrial bradycardia alternated with atrial arrhythmias, and heart rate was determined by ventricular escape rhythms. These findings extend the observation of bradycardia in tailcuff blood pressure measurements in A_3^{high} mice [6]. Our in vivo ECG recordings resemble those during severe forms of bradycardia–tachycardia syndrome. We found similar changes in isolated hearts of A_3^{high} mice, a setup that allows for assessment of the intrinsic heart rate [15]. This indicates that sinus nodal and AV nodal dysfunction of A_3^{high} hearts persists in the absence of autonomic regulation.

Atrial arrhythmias in A_3^{high} mice could either be due to intermittent activity of the sinus node, or afterdepolarizations and triggered activity [16–18] that may be provoked in A_3^{high} atria. Activation of IKACh (called also I_{KAdo}) by A_3AR receptor overexpression may also decrease the threshold of atrial tachyarrhythmias [19]. Further studies are needed to elucidate the mechanism of atrial tachycardias in A_3^{high} mice.

4.3. Attenuation of bradycardia and AV block during exercise

A_3^{high} overexpression caused bradycardia and AV block predominantly at rest (Figs. 1 and 2), with resumption of normal supraventricular rhythms during exercise. Of note is the fact that systemic infusion of β-adrenoreceptor agonists (orciprenaline) did not reverse atrial bradycardia in the isolated heart, suggestive of other heart rate-increasing factors in vivo (e.g., direct innervation of the sinus node or blockade of cholinergic receptors). In the present mouse model of chronic A_3^{high} overexpression, desensitization of A_3AR is possible. This may preferentially suppress Gi protein-dependent effects [22,23]. Receptor–ligand interaction studies have suggested that A_3AR may also act via Gq proteins [22,23] or through Rho [23,24], in addition to Gi protein-mediated effects caused by the "empty" receptor [25].

4.4. Differential regulation of heart rate and AV nodal function by A_1AR and A_3AR

A_1AR and A_3AR have different postreceptor signaling pathways: A_1ARs couple to Gi proteins that attenuate the effects of adrenergic stimulation [20,21]. Among other signaling pathways, A_3AR can interact with Rho and phospholipase D [24]. An important role for Rho in the postreceptor signaling of A_3^{high} mice is suggested by the similarities between the atrial phenotype of mice overexpressing a constitutively active form of Rho [26] and A_3^{high} mice.

Consistent with an attenuation of the response to catecholamines, overexpression of A_1 adenosine receptors causes a decreased chronotropic response to exercise, with little attenuation of resting heart rate [3]. Overexpression of A_3AR, in contrast, depresses heart rate preferentially at rest. AV nodal regulation appears to be similarly regulated: A_3 adenosine receptor overexpression, albeit at high levels, caused profound AV block predominantly at rest (Figs. 3 and 4), consistent with tonic depression of heart rate. A_1 adenosine receptor overexpression causes first-degree AV block that is not altered during exercise, but can be partially reversed by blockade of Gi proteins (Figs. 3 and 4 in Ref. [3]). Taken together, our findings suggest that A_3AR may be involved in the tonic regulation of heart rate and AV conduction, as has been suggested for the anti-ischemic action of A_3AR [27]. A_1AR may rather be involved in attenuation of adrenergic regulation of heart rate and AV conduction.

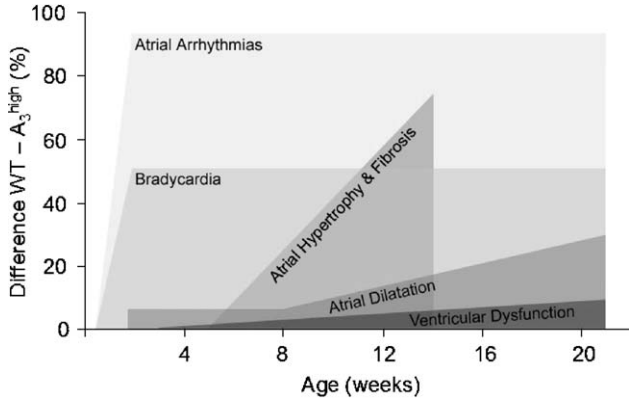

Fig. 6. Time course of the electrophysiological, structural, and contractile changes in A_3^{high} mice. Plotted are the relative differences in the measured parameters (ordinate, given in percent change of A_3^{high} and wild-type mice) vs. time (abscissa, in weeks). Bradycardia and atrial arrhythmias precede atrial and ventricular dysfunction and fibrosis, and atrial size markedly increases over time (see text for details).

4.5. Atrial arrhythmias pave the way for atrial and ventricular cardiomyopathy

Incessant atrial arrhythmias were present in juvenile A_3^{high} mice prior to atrial or ventricular dysfunction or structural remodeling. Furthermore, atrial size was only slightly increased in young mice and continued to increase with age, concomitant with atrial histological and biochemical changes suggestive of heart failure [28]. Fig. 6 summarizes the time course of electrophysiological, histological, biochemical, and contractile findings in this model. In the present study and in the previous report [6], ventricular myocardial disarray, dilatation, and altered function are present in A_3^{high} mice from the age of 14 weeks, with ventricular fibrosis not being evident up to the age of 28 weeks. Reduced SERCA expression at the age of 14 weeks in A_3^{high} mice is consistent with a previous report of decreased SERCA mRNA levels in the ventricles of A_3^{high} mice [6]. This may contribute to reduced force of contraction in isolated atria of A_3 high mice, in addition to a potential regulation of calcium release by A_3 adenosine receptors [29]. Our findings indicate that atrial and left ventricular dilatation and dysfunction in A_3^{high} mice develop over time and may be the morphological and functional reflections of a brady-cardiomyopathy. These findings are reminiscent of the ventricular hypertrophy and cardiomyopathy observed in dogs with chronic AV nodal block [30] and suggestive of an atrial form of "brady-cardiomyopathy" that over time also extends to the ventricular level.

Atrial dilatation may occur in mice without concurrent arrhythmias [31]. Atrial hypertrophy may be accompanied by heart block [32], and atrial dilatation may precede atrial fibrillation in mice [33]. In other transgenic mouse models, both atrial dilatation and atrial fibrillation, or atrial dilatation and diverse forms of sinus and AV nodal dysfunction have been reported [26,32–34]. An association of atrial arrhythmias, atrial enlargement, and atrial fibrosis has been reported in mice with high-level heart-directed overexpression of RhoA [26] or junctin [34], but the time course of these alterations has not been studied. Atrial brady-cardiomyopathy in A_3^{high} mice (i.e., atrial arrhythmias preceding atrial and ventricular mechanical dysfunction) is therefore, to the best of our knowledge, a novel finding.

4.6. Implications

Cardiac expression of A_3AR alters the electrophysiological function of both the sinus node and AV nodal function in vivo. In contrast to our findings in A_1AR-overexpressing mice, A_3AR overexpression predominantly suppresses heart rate during periods of low autonomic tone in vivo.

Some of the ventricular hemodynamic and structural changes reported in the initial characterization of A_3^{high} mice [6] may have been a consequence of cardiac arrhythmias.

Enhanced expression or function of adenosine receptors has been suggested as a target for gene therapy to prevent postischemic myocardial damage [6,35]. Although differences in rate, ionic currents, and size between murine and human hearts implicate caution when transferring results to the clinical setting, our data suggest that high-level overexpression of A_3AR may adversely affect atrial electrophysiology. The potential benefits notwithstanding, careful targeting and dosing accompanied by a complete cardiovascular evaluation is necessary to obtain a maximal level of safety for gene therapy aimed at enhancing expression or function of adenosine receptors.

Acknowledgements

The authors would like to thank Daniela Holtmannspötter and Marcel Tekook for excellent technical assistance. L.F. is a fellow of the Emmy Noether-Programm of the Deutsche Forschungsgemeinschaft. This work was supported by the Deutsche Forschungsgemeinschaft as part of the Sonderforschungsbereich 556 "Heart failure and arrhythmias" (to P.K., L.F., and J.N.) and by the IZKF Münster (project ZPG4, to P.K.).

We—obviously excluding G.B.—would like to dedicate this work to the 60th birthday of Günter Breithardt MD., in February 2004.

References

[1] DiFrancesco D. The onset and autonomic regulation of cardiac pacemaker activity: relevance of the f current. Cardiovasc Res 1995;29:449–56.

[2] Wainger BJ, DeGennaro M, Santoro B, Siegelbaum SA, Tibbs GR. Molecular mechanism of cAMP modulation of HCN pacemaker channels. Nature 2001;411:805–10.

[3] Kirchhof P, Fabritz CL, Fortmüller L, et al. Decreased chronotropic response to exercise and atrio-ventricular nodal conduction delay in mice overexpressing the A1-adenosine receptor. Am J Physiol 2003; 285:H145–53.
[4] Salvatore CA, Jacobson MA, Taylor HE, Linden J, Johnson RG. Molecular cloning and characterization of the human A_3 adenosine receptor. Proc Natl Acad Sci U S A 1993;90:10365–9.
[5] Carr CS, Hill RJ, Masamune H, et al. Evidence for a role for both the adenosine A1 and A3 receptors in protection of isolated human atrial muscle against simulated ischaemia. Cardiovasc Res 1997;36:52–9.
[6] Black Jr RG, Guo Y, Ge ZD, et al. Gene dosage-dependent effects of cardiac-specific overexpression of the A_3 adenosine receptor. Circ Res 2002;91:165–72.
[7] Maddock HL, Mocanu MM, Yellon DM. Adenosine A(3) receptor activation protects the myocardium from reperfusion/reoxygenation injury. Am J Physiol, Heart Circ Physiol 2002;283:H1307–13.
[8] Cross HR, Murphy E, Black RG, Auchampach J, Steenbergen C. Overexpression of A(3) adenosine receptors decreases heart rate, preserves energetics, and protects ischemic hearts. Am J Physiol, Heart Circ Physiol 2002;283:H1562–8.
[9] Kramer K, van Acker SA, Voss HP, et al. Use of telemetry to record electrocardiogram and heart rate in freely moving mice. J Pharmacol Toxicol Methods 1993;30:209–15.
[10] Cogliati T, Good DJ, Haigney M, et al. Predisposition to arrhythmia and autonomic dysfunction in Nhlh1-deficient mice. Mol Cell Biol 2002;22:4977–83.
[11] Fabritz L, Kirchhof P, Franz MR, et al. Prolonged action potential durations, increased dispersion of repolarization, and polymorphic ventricular tachycardia in a mouse model of proarrhythmia. Basic Res Cardiol 2003;98:25–32.
[12] Fabritz L, Kirchhof P, Franz MR, et al. Effect of pacing and mexiletine on dispersion of repolarisation and arrhythmias in hearts of SCN5A ð-KPQ (LQT3) mice. Cardiovasc Res 2003;57: 1085–93.
[13] Neumann J, Boknik P, Matherne GP, Lankford AR, Schmitz W. Pertussis toxin sensitive and insensitive effects of adenosine and carbachol in murine atria overexpressing A(1)-adenosine receptors. Br J Pharmacol 2003;138:209–17.
[14] Neumann J, Boknik P, DePaoli-Roach A, et al. Targeted overexpression of phospholamban to mouse atrium depresses Ca^{2+} transport and contractility. J Mol Cell Cardiol 1998;30:1991–2002.
[15] Jose AD, Collison D. The normal range and determinants of the intrinsic heart rate in man. Cardiovasc Res 1970;4:160–7.
[16] Belardinelli L, Shryock JC, Song Y, Wang D, Srinivas M. Ionic basis of the electrophysiological actions of adenosine on cardiomyocytes. FASEB J 1995;9:359–65.
[17] Wu L, Belardinelli L, Zablocki JA, Palle V, Shryock JC. A partial agonist of the A(1)-adenosine receptor selectively slows AV conduction in guinea pig hearts. Am J Physiol, Heart Circ Physiol 2001;280: H334–43.
[18] Song Y, Wu L, Shryock JC, Belardinelli L. Selective attenuation of isoproterenol-stimulated arrhythmic activity by a partial agonist of adenosine A1 receptor. Circulation 2002;105:118–23.
[19] Workman AJ, Kane KA, Rankin AC. Ionic basis of a differential effect of adenosine on refractoriness in rabbit AV nodal and atrial isolated myocytes. Cardiovasc Res 1999;43:974–84.
[20] Gupta RC, Neumann J, Durant P, Watanabe AM. A1-adenosine receptor-mediated inhibition of isoproterenol-stimulated protein phosphorylation in ventricular myocytes. Evidence against a cAMP-dependent effect. Circ Res 1993;72:65–74.
[21] Headrick JP, Gauthier NS, Morrison RR, Matherne GP. Chronotropic and vasodilatory responses to adenosine and isoproterenol in mouse heart: effects of adenosine A1 receptor overexpression. Clin Exp Pharmacol Physiol 2000;27:185–90.
[22] Palmer TM, Benovic JL, Stiles GL. Agonist-dependent phosphorylation and desensitization of the rat A_3 adenosine receptor. Evidence for a G-protein-coupled receptor kinase-mediated mechanism. J Biol Chem 1995;270:29607–13.
[23] Palmer TM, Gettys TW, Stiles GL. Differential interaction with and regulation of multiple G-proteins by the rat A_3 adenosine receptor. J Biol Chem 1995;270:16895–902.
[24] Mozzicato S, Joshi BV, Jacobson KA, Liang BT. Role of direct RhoaA-phospholipase D interaction in mediating adenosine-induced protection from cardiac ischemia. FASEB J; 2003.
[25] Milano C, Allen L, Rockman HA, et al. Enhanced myocardial function in transgenic mice overexpressing the beta 2-adrenergic receptor. Science 1994;264:582–6.
[26] Sah VP, Minamisawa S, Tam SP, et al. Cardiac-specific overexpression of RhoA results in sinus and atrioventricular nodal dysfunction and contractile failure. J Clin Invest 1999;103:1627–34.
[27] Liang BT, Jacobson KA. A physiological role of the adenosine A3 receptor: sustained cardioprotection. Proc Natl Acad Sci U S A 1998; 95:6995–9.
[28] Frank KF, Bolck B, Erdmann E, Schwinger RH. Sarcoplasmic reticulum Ca(2+)-ATPase modulates cardiac contraction and relaxation. Cardiovasc Res 2003;57:20–7.
[29] Zucchi R, Yu G, Ghelardoni S, Ronca F, Ronca-Testoni S. A_3 adenosine receptor stimulation modulates sarcoplasmic reticulum Ca(2+) release in rat heart. Cardiovasc Res 2001;50:56–64.
[30] Volders PG, Sipido KR, Vos MA, et al. Cellular basis of biventricular hypertrophy and arrhythmogenesis in dogs with chronic complete atrioventricular block and acquired torsade de pointes. Circulation 1998;98:1136–47.
[31] Hunter JJ, Tanaka N, Rockman HA, Ross Jr J, Chien KR. Ventricular expression of a *MLC-2v-ras* fusion gene induces cardiac hypertrophy and selective diastolic dysfunction in transgenic mice. J Biol Chem 1995;270:23173–8.
[32] Hein L, Stevens ME, Barsh GS, et al. Overexpression of angiotensin AT1 receptor transgene in the mouse myocardium produces a lethal phenotype associated with myocyte hyperplasia and heart block. Proc Natl Acad Sci U S A 1997;94:6391–6.
[33] Kirchhof P, Fabritz L, Neumann J, Schmitz W, Müller FU. A mouse model of spontaneous atrial fibrillation: overexpression of a human cardiac isoform of CREM (Abstract). Einthoven Symposium, Leiden, NL; 2002.
[34] Hong CS, Cho MC, Kwak YG, et al. Cardiac remodeling and atrial fibrillation in transgenic mice overexpressing junctin. FASEB J 2002; 16:1310–2.
[35] Matherne GP, Linden J, Byford AM, Gauthier NS, Headrick JP. Transgenic A-1 adenosine receptor overexpression increases myocardial resistance to ischemia. PNAS 1997;94:6541–6.